Thermochimica Acta 695 (2021) 178807

Contents lists available at ScienceDirect

Thermochimica Acta

journal homepage: www.elsevier.com/locate/tca

Short communication

Low intrinsic thermal conductivity of Spark Plasma Sintered dense $KNbO_3$ and $NaNbO_3$ perovskite ceramics

F. Delorme [a,*], C. Chen [a], F. Schoenstein [b], N. Jaber [a], F. Jean [a], M. Bah [a], Q. Simon [a], T. Chartier [a], P. Laffez [a], I. Monot-Laffez [a], F. Giovannelli [a]

[a] Université de Tours, CNRS, INSA CVL, GREMAN UMR 7347, IUT de Blois, 15 rue de la chocolaterie, CS 2903, F-41029, Blois Cedex, France
[b] Université Paris 13, Sorbonne Paris Nord, Laboratoire des Sciences des Procédés et des Matériaux - LSPM, CNRS, UPR 3407, 99 avenue Jean Baptiste Clément, F-93430, Villetaneuse, France

ARTICLE INFO

Keywords:
Spark plasma sintering
Ceramics
Perovskite
Thermal conductivity

ABSTRACT

The origin of low thermal conductivity in niobium-containing perovskites was investigated. Therefore, dense $NaNbO_3$ and $KNbO_3$ ceramics were sintered by spark plasma sintering. The grain size was in the 1–10 μm range. $NaNbO_3$ ceramic has shown a stable thermal conductivity circa 2.6 W m^{-1} K^{-1} from 373 to 1000 K and $KNbO_3$, values from 2.5 to a plateau at 1.2 W m^{-1} K^{-1} since 673 K. This value is the lowest thermal conductivity reported for an oxide presenting a perovskite structure. The origin of such low thermal conductivities is indicated to be related with cation deficiency on the A-site of the niobium-containing perovskites.

1. Introduction

Thermoelectric materials can contribute to limit global warming by directly transforming heat into electricity without any emissions (CO_2, other gases, radiations, …), vibrations or moving parts [1]. Thermoelectric materials potential is evaluated by the thermoelectric figure of merit $ZT = S^2\sigma T/\kappa = PF\ T/\kappa$, where T is the absolute temperature, S the Seebeck coefficient, σ the electrical conductivity, κ the thermal conductivity and PF the power factor. However, the three parameters, S, σ and κ, are strongly interconnected through more fundamental physical parameters.

Therefore, trying to discover new high ZT thermoelectric materials is a very active research field [2–10] as well as trying to improve ZT values of known materials [11–18]. Gaultois et al. [19] have shown from element abundance and Herfindahl-Hirschman indices for production and reserve criteria that only three families of materials are suitable for mass production: highly conductive transition metal oxides, silicides with low bismuth content, and some half-Heusler compounds.

Oxides are considered as potential thermoelectric materials since 1997, when Terasaki et al. [20] reported a high power factor in Na_xCoO_2. Nowadays, the best reported values for n-type oxides are ZT = 0.67 at 773 K [21] in $CaMnO_3$-based perovskite materials, ZT = 0.6 at 1000 K [22] in $SrTiO_3$-based perovskite materials, and for p-type oxides the best ZT values are exhibited in $Ca_3Co_4O_9$-based materials (ZT = 0.74 at 800 K [23]).

However, one of the main issues of oxides compared to other thermoelectric materials is their relatively high thermal conductivity. Therefore, many routes to reduce their thermal conductivity have been investigated, such as substitutions by heavier elements, nanostructuring, composites, porosity, microcracking, … [24–40].

The $(K_{0.5}Na_{0.5})NbO_3$ perovskite is a widely studied lead-free alternative to lead-zirconate-titanates piezoceramics since 2004 [41–45]. However, Delorme et al. [46] have reported promising thermoelectric properties in $(K_{0.5}Na_{0.5})NbO_3$ perovskite sintered by spark plasma sintering (SPS) due to oxygen non-stoichiometry. The most interesting feature is that thermal conductivity is stable from 325 to 1000 K between 3.5 and 4 W m^{-1} K^{-1} which is far lower than the values reported in the largely studied $SrTiO_3$ perovskite (circa 10 W m^{-1} K^{-1} at room temperature) [47]. Several phenomena can contribute to such low values. For instance, A-site deficiency in $SrTiO_3$ perovskite was found to reduce thermal conductivity [47–49]. The volatility of alkali metals is well known and it is difficult to avoid when sintering $(K_{0.5}Na_{0.5})NbO_3$ ceramics [45]. To reach thermal conductivities circa 4 W m^{-1} K^{-1} in $SrTiO_3$ perovskite, it requires almost 20 % vacancies [49]. However, $(K_{0.5}Na_{0.5})NbO_3.\delta$ ceramics have shown (Na + K)/Nb ratios higher than 0.9 [45]. Moreover, the $(K_{0.5}Na_{0.5})NbO_3$ composition is close to the morphotropic phase boundary that can lead to the formation of domains with A-site cationic heterogeneity [50] that could contribute to reduce

* Corresponding author at: French-German research Institute of Saint-Louis, 5 rue du Général Cassagnou, BP 70034, F-68301, Saint-Louis Cedex, France.
E-mail address: fabian.delorme@isl.eu (F. Delorme).

https://doi.org/10.1016/j.tca.2020.178807
Received 20 August 2020; Received in revised form 20 October 2020; Accepted 21 October 2020
Available online 24 October 2020

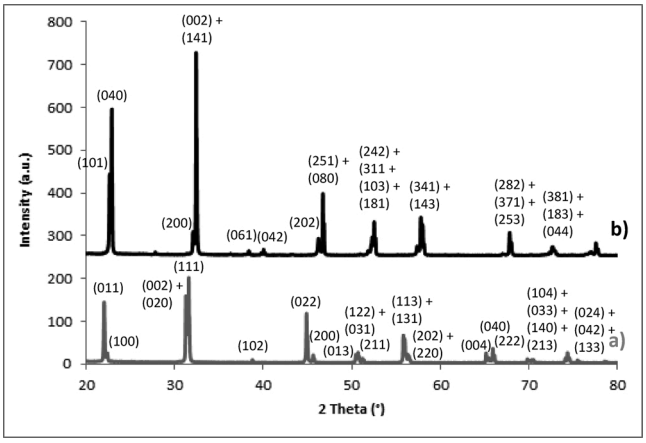

Fig. 1. XRD patterns of the a) $KNbO_3$ ceramic and b) $NaNbO_3$ ceramic.

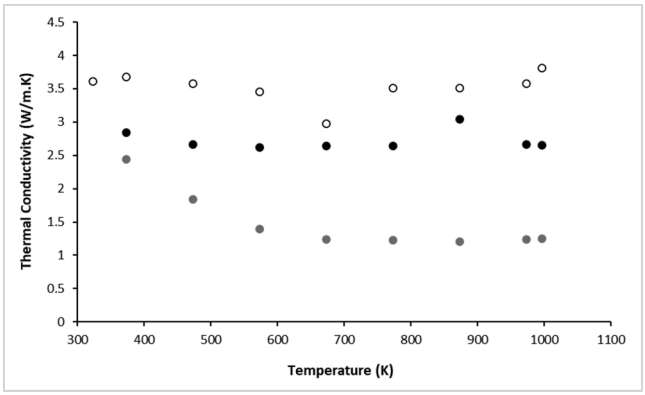

Fig. 2. Temperature dependence of the thermal conductivity of $(K_{0.5}Na_{0.5})NbO_3$ (o), $NaNbO_3$ (•) and $KNbO_3$ (•) ceramics.

thermal conductivity. Finally, ferroelectric domains have also been reported in $(K_{0.5}Na_{0.5})NbO_3$ perovskite [51].

Therefore, in order to investigate the origin of the low thermal conductivity of $(K_{0.5}Na_{0.5})NbO_3$ ceramics, dense $KNbO_3$ and $NaNbO_3$ ceramics, representing the end members of the solid solution, have been sintered by Spark Plasma Sintering and characterized. Indeed, it is well known that high density $KNbO_3$ and $NaNbO_3$ ceramics are difficult to sinter due to the volatility of the alkali metals at relatively low temperatures [52,53].

2. Materials and methods

$KNbO_3$ and $NaNbO_3$ samples were synthesised from K_2CO_3 (Chempur, ≥ 99 % purity), Na_2CO_3 (Chempur, ≥ 99.9 % purity) and Nb_2O_5 (Chempur, ≥ 99.9 % purity) precursors. The precursors were heated at 200 °C for 4 h and then stoichiometric amounts of the precursors were mixed for 5 min at 400 rpm in an agate planetary ball mill (Retsch PM 100). The powders were then heated at 830 °C for 12 h at a rate of 2 °C/min, in an alumina crucible and slowly cooled down to room temperature.

Sintering was performed by Spark Plasma Sintering (Syntex 515 S of the SPS Platform Ile-de-France). The synthesised powders were placed in a 15 mm diameter graphite die. A graphite foil was placed between the samples and the different parts of the die. Experiments were performed in argon atmosphere. $NaNbO_3$ sample was first sintered using conditions close to the ones reported by Wada et al. [52]: 1200 °C and 50 MPa. However, the experiment was stopped circa 1045 °C as a liquid phase appeared. Therefore, both $NaNbO_3$ and $KNbO_3$ ceramics were sintered using the cycle developed for $(K_{0.5}Na_{0.5})NbO_3$-δ ceramics [46]: a pressure of 50 MPa was applied whereas the temperature was raised at 100 °C/min up to 920 °C for 5 min. Then the samples were cooled down to room temperature at 100 °C/min.

Graphite foils used during the SPS process were removed by polishing. The pellets were cut into 2.8 × 2.8 × 13 and 6 × 6 × 1 mm parallelepipeds with a diamond wire saw for electrical and thermal properties measurements, respectively.

Weight and dimensions of the samples used for thermoelectric characterization were used to calculate apparent density of the samples.

Resistivity and Seebeck coefficient were measured simultaneously in a ZEM III equipment (ULVAC Technologies) from 1000 to 325 K. The laser flash diffusivity technique (Netzsch LFA 457) from 373 to 1000 K under vacuum after graphite coating was used to measure thermal diffusivity. Each sample was measured three times at each temperature. The specific heat capacity (c_p) was measured by differential scanning calorimetry (Netzsch STA 449 F3 Jupiter) from 330 to 1000 K, with a heating rate of 20 K.min^{-1} in platinum crucibles and in nitrogen atmosphere.

Powder X-ray diffraction (XRD) patterns have been recorded at room temperature on a BRUKER D8 Advance θ/2θ diffractometer (Cu-K_α radiation, at 40 kV and 40 mA) with a Linxeye detector from 20 to 80°(2θ) with a step of 0.02° and a counting time of 0.5 s per step.

Samples were first gold coated and then observed by scanning electron microscopy (SEM - Tescan Mira 3 field emission microscope coupled with an Energy Dispersive Spectrometer EDS Oxford INCA X-Act).

3. Results and discussion

After sintering, the two pellets are greyish, $NaNbO_3$ being darker than $KNbO_3$.

Fig. 1 exhibits the XRD patterns measured on the ceramic pellets after sintering by SPS. All the peaks can be attributed to the $KNbO_3$ (PDF 01-071-0946) and $NaNbO_3$ (PDF 00-033-1270) compounds.

The relative densities calculated from the theoretical value given by PDF cards are high and similar, 96 and 97 % for $KNbO_3$ and $NaNbO_3$, respectively. The value for $NaNbO_3$ is consistent with the recent results reported by Gouget et al. [54]: indeed, they achieved densities of at least 94 % for samples sintered by SPS at 900 °C and 100 MPa during 5 min.

Temperature dependence of the thermal conductivity of the $(K_{0.5}Na_{0.5})NbO_3$, $KNbO_3$ and $NaNbO_3$ ceramics sintered by SPS, from 373 to 1000 K is shown in Fig. 2. As already reported [46], thermal conductivity of $(K_{0.5}Na_{0.5})NbO_3$ ceramic is stable (3.5−4 W m^{-1} K^{-1}) over the whole temperature range and lower than the thermal conductivity of conventionally studied $SrTiO_3$ perovskite [47]. $NaNbO_3$ ceramic presents a similar behaviour, i.e. stable over the whole temperature range, but a lower thermal conductivity value circa 2.6 W m^{-1} K^{-1}. $KNbO_3$ ceramic presents a different behaviour, similar to $SrTiO_3$ one. The highest thermal conductivity is observed around room temperature and decreases until it reaches a plateau. The value at 373 K is below 2.5 W m^{-1} K^{-1} and the plateau value (1.2 W m^{-1} K^{-1}) is reached at 673 K. As far as the authors know, this is the lowest thermal conductivity reported for an oxide presenting a perovskite structure. Moreover, this value is lower than the thermal conductivity of oxides used as thermal barriers, like yttrium-stabilized zirconia or pyrochlores [55].

The three niobium-containing perovskites exhibit low thermal conductivity values. Therefore, it excludes the possibility that the origin of low thermal conductivity values in $(K_{0.5}Na_{0.5})NbO_3$ ceramics could be related to composition heterogeneities due to the vicinity of the morphotropic phase boundary. Indeed, pure poles as $KNbO_3$ and $NaNbO_3$ cannot present such domains.

An influence of the different crystallographic structures has been ruled out by Delorme et al. [46]. Indeed, in $K_{0.5}Na_{0.5}NbO_3$, thermal conductivity remains similar whereas the perovskite is orthorhombic, tetragonal and cubic at room temperature, 450 K and 700 K,

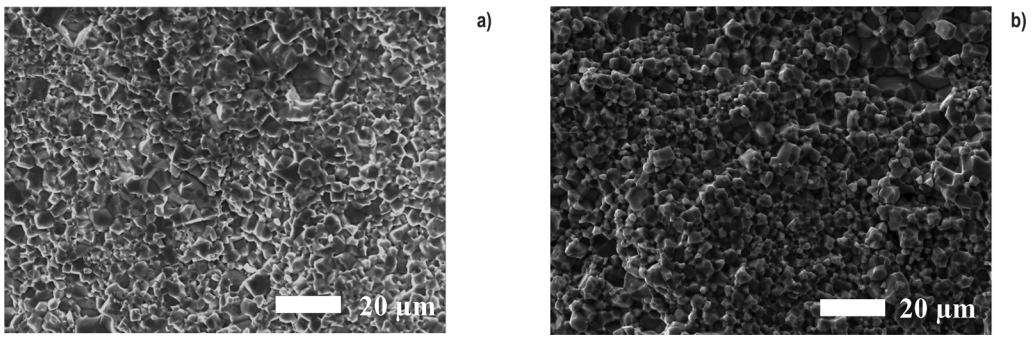

Fig. 3. SEM images of a) $NaNbO_3$ and b) $KNbO_3$ ceramics.

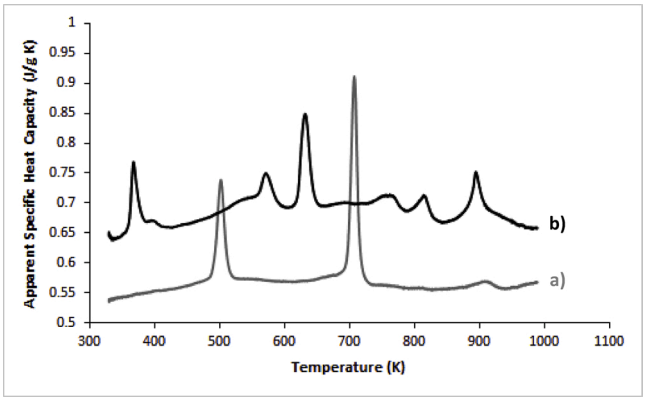

Fig. 4. Temperature dependence of apparent specific heat capacity of a) $KNbO_3$ and b) $NaNbO_3$ ceramics.

respectively. Similarly, no significant thermal conductivity change related to phase transitions can be observed in $NaNbO_3$ and $KNbO_3$

Another, possibility could be nanosized grains [27,35,37]. However, SEM observations (Fig. 3) show that both $KNbO_3$ and $NaNbO_3$ ceramics exhibit micrometer-sized grains. According to Bah et al. [45], $(K_{0.5}Na_{0.5})NbO_3$ ceramics sintered by SPS exhibits micrometer-sized grains too. Therefore, the low thermal conductivities of niobium-containing perovskite are not related to nanograins. However, EDS measurements show that $(K_{0.5}Na_{0.5})NbO_3$, $KNbO_3$ and $NaNbO_3$ ceramics present a common feature : they all present a cation deficiency on the A-site of the perovskite. A decrease in the thermal conductivity due to A-site deficiency has already been reported for $SrTiO_3$ perovskite [47–49]. However, the thermal conductivity values obtained in niobium-containing perovskites are lower than those obtained in $SrTiO_3$ even with higher deficiency. Indeed, the (Na + K)/Nb ratio is circa 0.97, 0.91 and 0.96 for $(K_{0.5}Na_{0.5})NbO_3$, $KNbO_3$ and $NaNbO_3$, respectively. It appears that the lower the (Na + K)/Nb ratio, the lower the thermal conductivity. Therefore, one can conclude that the A-deficiency is responsible for the low thermal conductivity measured in niobium-containing perovskites.

Such low thermal conductivities make $KNbO_3$ and $NaNbO_3$ ceramics potentially attractive for thermal barrier applications. However, for such application, an absence of phase transition in the targeted temperature range and chemical inertness is requested [56–58].

The thermal diffusivity and c_p values measured circa room temperature on the SPS-sintered $KNbO_3$ ceramics are consistent with the values reported for single crystals by Hofmeister [59]. Fig. 4 exhibits the temperature dependence of apparent specific heat capacity values of $KNbO_3$ and $NaNbO_3$ ceramics from 330 to 1000 K. For $KNbO_3$, two peaks can be observed at circa 486 and 693 K, corresponding to orthorhombic-tetragonal and tetragonal-cubic phase transitions, respectively [59,60]. Temperature-resolved XRD studies should allow determining whether these phase transitions are associated with the volume changes that could be detrimental for thermal barrier application.

$NaNbO_3$ cannot probably be used for thermal barrier application as it is well known to present many phase transitions [54,61–63]. Fig. 4 shows that for $NaNbO_3$, at least six peaks can be observed at 352 (with a shoulder after the peak), 554 (with a shoulder prior the peak), 612, 730, 790, 850 with a shoulder around 920 K, respectively. However, discussing the correlation between peaks and phase transitions in $NaNbO_3$ is far beyond this communication's aim.

Finally, thermoelectric properties have been measured. Indeed, according to the thermoelectric figure of merit $ZT = S^2\sigma T/\kappa$, ceramics with low thermal conductivity can present promising thermoelectric properties as reported for $(K_{0.5}Na_{0.5})NbO_3$-δ ceramics [46]. Theoretical study [64] has shown that $NaNbO_3$ and in a larger extent $KNbO_3$ could present high thermoelectric properties, if appropriately doped (i.e. controlled oxygen stoichiometry and divalent substitution on the of alkali metal site). Unfortunately, it was impossible to measure the electrical conductivity and Seebeck coefficient of $KNbO_3$ ceramic in ZEM3. Indeed, the 2.8 × 2.8 × 13 mm bar broke when clamped between the ZEM3 electrodes, suggesting that $KNbO_3$ is a fragile material. For $NaNbO_3$ ceramic, the properties were only measurable at 1000 K. The Seebeck coefficient value is -688 µV K^{-1}, indicating a n-type material. This value is similar to the one reported for $(K_{0.5}Na_{0.5})NbO_3$-δ ceramics [46]. Unfortunately, the electrical conductivity is limited at 16 S m^{-1}, which is about one fifth of the value reported for $(K_{0.5}Na_{0.5})NbO_3$-δ ceramics [46]. It will be necessary to optimize the power factor by doping and control of the oxygen stoichiometry to estimate the real potential of niobium-containing perovskites as thermoelectric materials.

4. Conclusion

Dense $NaNbO_3$ and $KNbO_3$ ceramics were obtained by spark plasma sintering. After sintering, the two pellets are greyish, indicating an oxygen deficiency as $(K_{0.5}Na_{0.5})NbO_3$-δ when sintered under the similar conditions. The grain size was in the 1–10 µm range. Both $NaNbO_3$ and $KNbO_3$ ceramics present low thermal conductivity: circa 2.6 W m^{-1} K^{-1} and stable from 373 to 1000 K for $NaNbO_3$ and from 2.5 to 1.2 W m^{-1} K^{-1} since 673 K for $KNbO_3$. This value is the lowest thermal conductivity reported for an oxide presenting a perovskite structure and is lower than the thermal conductivity of oxides used as thermal barriers, like yttrium-stabilized zirconia or pyrochlores. The origin of such low thermal conductivities is indicated to be related with cation deficiency on the A-site of the perovskite. Indeed, the (Na + K)/Nb ratio is circa 0.97, 0.91 and 0.96 for $(K_{0.5}Na_{0.5})NbO_3$, $KNbO_3$ and $NaNbO_3$, respectively. Applications in the field of thermal barriers or as thermoelectric materials could be expected. However, one would require the absence of phase transitions with important volume changes and the other, optimizing the electrical properties by controlling the charge carrier concentration by doping or controlled oxygen deficiency, respectively.

CRediT authorship contribution statement

F. Delorme: Conceptualization, Investigation, Visualization, Writing - original draft, Writing - review & editing. **C. Chen:** Investigation, Visualization, Writing - review & editing. **F. Schoenstein:** Investigation, Writing - review & editing. **N. Jaber:** Investigation. **F. Jean:** Investigation. **M. Bah:** Validation, Writing - review & editing. **Q. Simon:** Conceptualization, Validation, Writing - review & editing. **T. Chartier:** Investigation. **P. Laffez:** Conceptualization, Validation, Writing - review & editing, Supervision. **I. Monot-Laffez:** Conceptualization, Validation, Writing - review & editing, Supervision. **F. Giovannelli:** Conceptualization, Investigation, Validation, Writing - review & editing, Supervision.

Declaration of Competing Interest

The authors declare that they have no known competing financial interests or personal relationships that could have appeared to influence the work reported in this paper.

Acknowledgements

This research did not receive any specific grant from funding agencies in the public, commercial, or not-for-profit sectors.

References

[1] J.W. Fergus, Oxide materials for high temperature thermoelectric energy conversion, J. Eur. Ceram. Soc. 32 (2012) 525–540.
[2] K.F. Hsu, S. Loo, F. Guo, W. Chen, J.S. Dyck, C. Uher, T. Hogan, E. K. Polychroniadis, M.G. Kanatzidis, Cubic $AgPb_mSbTe_{2+m}$: bulk thermoelectric materials with high figure of merit, Science 303 (2004) 818–821.
[3] J.R. Sootsman, D.Y. Chung, M.G. Kanatzidis, New and old concepts in thermoelectric materials, Angew. Chem. Int. Ed. 48 (2009) 8616–8639.
[4] L.-D. Zhao, S.-H. Lo, Y. Zhang, H. Sun, G. Tan, C. Uher, C. Wolverton, V.P. Dravid, M.G. Kanatzidis, Ultralow thermal conductivity and high thermoelectric figure of merit in SnSe crystals, Nature 508 (2014) 373–377.
[5] T. Barbier, P. Lemoine, S. Gascoin, O.I. Lebedev, A. Kaltzoglou, P. Vaqueiro, A. V. Powell, R.I. Smith, E. Guilmeau, Structural stability of the synthetic thermoelectric ternary and nickel-substituted tetrahedrite phases, J. Alloys. Compd. 634 (2015) 253–262.
[6] F. Delorme, C. Chen, B. Pignon, F. Schoenstein, L. Perrière, F. Giovannelli, Promising high temperature thermoelectric properties of dense $Ba_2Co_9O_{14}$ ceramics, J. Eur. Ceram. Soc. 37 (2017) 2615–2620.
[7] C. Chen, F. Giovannelli, M. Zaghrioui, L. Perrière, F. Delorme, Synthesis, sintering, transport and thermal properties of $Na_2Fe_2Ti_6O_{16}$ freudenbergite, Mater. Chem. Phys. 198 (2017) 1–6.
[8] S.A. Miller, P. Gorai, B.R. Ortiz, A. Goyal, D. Gao, S.A. Barnett, T.O. Mason, G. J. Snyder, Q. Lv, V. Stevanovic, E.S. Toberer, Capturing anharmonicity in a lattice thermal conductivity model for high-throughput predictions, Chem. Mater. 29 (2017) 2494–2501.
[9] C. Chen, F. Giovannelli, J.R. Duclère, F. Delorme, Thermoelectric properties of $Fe_2Ti_{1-x}Nb_xO_5$ pseudobrookite ceramics with low thermal conductivity, J. Eur. Ceram. Soc. 37 (2017) 4681–4685.
[10] C. Chen, F. Delorme, F. Schoenstein, M. Zaghrioui, D. Flahaut, J. Allouche, F. Giovannelli, Synthesis, sintering and thermoelectric properties of $Co_{1-x}M_xO$ (M = Na, $0 \leq x \leq 0.07$; M = Ag, $0 \leq x \leq 0.05$), J. Eur. Ceram. Soc. 39 (2019) 346–351.
[11] J.P. Heremans, C.M. Thrush, D.T. Morelli, Thermopower enhancement in lead telluride nanostructures, Phys. Rev. B 70 (2004), 115334.
[12] H. Odahara, O. Yamashita, K. Satou, S. Tomiyoshi, J.-I. Tani, H. Kido, Increase of the thermoelectric power factor in Cu/Bi/Cu, Ni/Bi/Ni, and Cu/Bi/Ni composite materials, J. Appl. Phys. 97 (2005), 103722.
[13] B.C. Sales, Critical overview of recent approaches to improved thermoelectric materials, Int. J. Appl. Ceram. Technol. 4 (2007) 291–296.
[14] D.L. Medlin, G.J. Snyder, Interfaces in bulk thermoelectric materials, Curr. Opin. Colloid Interf. Sci. 14 (2009) 226–235.
[15] C.J. Vineis, A. Shakouri, A. Majumdar, M.G. Kanatzidis, Nanostructured thermoelectric: big efficiency gains from small features, Adv. Mater. 22 (2010) 3970–3980.
[16] N.V. Nong, C.-J. Liu, M. Ohtaki, Improvement on the high temperature thermoelectric performance of Ga-doped misfit-layered $Ca_3Co_{4-x}Ga_xO_{9+\delta}$ (x = 0, 0.05, 0.1, and 0.2), J. Alloys. Compd. 491 (2010) 53–56.
[17] M. Zebarjadi, G. Joshi, G. Zhu, B. Yu, A. Minnich, Y. Lan, X. Wang, M. Dresselhaus, Z. Ren, G. Chen, Power factor enhancement by modulation doping in bulk nanocomposites, Nano Lett. 11 (2011) 2225–2230.
[18] M.A. Torres, F.M. Costa, D. Flahaut, K. Touati, S. Rasekh, N.M. Ferreira, J. Allouche, M. Depriester, M.A. Madre, A.V. Kovalevsky, J.C. Diez, A. Sotelo, Significant enhancement of the thermoelectric performance in $Ca_3Co_4O_9$ thermoelectric materials through combined strontium substitution and hot-pressing process, J. Eur. Ceram. Soc. 39 (2019) 1186–1192.
[19] M.W. Gaultois, T.D. Sparks, C.K.H. Borg, R. Seshadri, W.D. Bonificio, D.R. Clarke, Data-driven review of thermoelectric materials: performance and resource considerations, Chem. Mater. 25 (2013) 2911–2920.
[20] I. Terasaki, Y. Sasago, K. Uchinokura, Large thermoelectric power in $NaCo_2O_4$ single crystals, Phys. Rev. B 56 (1997) R12685–R12687.
[21] X. Song, S.A. Paredes Navia, L. Liang, C. Boyle, C.-O. Romo-De-La-Cruz, B. Jackson, A. Hinerman, M. Wilt, J. Prucz, Y. Chen, Grain boundary phase segregation for dramatic improvement of the thermoelectric performance of oxide ceramics, ACS Appl. Mater. Interfaces 10 (2018) 39018–39024.
[22] J. Wang, B.-Y. Zhang, H.-J. Kang, Y. Li, X. Yaer, J.-F. Li, Q. Tan, S. Zhang, G.-H. Fan, C.-Y. Liu, L. Mioa, D. Nan, T.-M. Wang, L.-D. Zhao, Record high thermoelectric performance in bulk $SrTiO_3$ via nano-scale modulation doping, Nano Energy 35 (2017) 387–395.
[23] S. Saini, H.S. Yaddanapudi, K. Tian, Y. Yin, D. Magginetti, A. Tiwari, Terbium ion doping in $Ca_3Co_4O_9$: a step towards high-performance thermoelectric materials, Sci. Rep. 7 (2017) 44621.
[24] D. Wang, L. Chen, Q. Wang, J. Li, Fabrication and thermoelectric properties of $Ca_{3-x}Dy_xCo_4O_{9+\delta}$ system, J. Alloys. Compd. 376 (2004) 58–61.
[25] J. Noudem, S. Lemonnier, M. Prevel, E.S. Reddy, E. Guilmeau, C. Goupil, Thermoelectric ceramics generators, J. Eur. Ceram. Soc. 28 (2008) 41–48.
[26] Y. Wang, Y. Sui, J. Cheng, X. Wang, W. Su, Comparison of the high temperature thermoelectric properties for Ag-doped and Ag-added Ca_3Co_4O9, J. Alloys. Compd. 477 (2009) 817–821.
[27] K. Koumoto, Y. Wang, R. Zhang, A. Kosuga, R. Funahashi, Oxide thermoelectric materials: a nanostructuring approach, Annu. Rev. Mater. Res. 40 (2010) 363.
[28] F. Delorme, C. Fernandez Martin, P. Marudhachalam, D. Ovono Ovono, G. Guzman, Effect of Ca substitution by Sr on the thermoelectric properties of $Ca_3Co_4O_9$ ceramics, J. Alloys. Compd. 509 (2011) 2311–2315.
[29] N.V. Nong, C.-J. Liu, M. Ohtaki, High-temperature thermoelectric properties of late rare earth-doped $Ca_3Co_4O9+\delta$, J. Alloys. Compd. 509 (2011) 977–981.
[30] M. Ohtaki, S. Miyaishi, Extremely low thermal conductivity in oxides with cage-like crystal structure, J. Electron. Mater. 42 (2013) 1299.
[31] Y. Zhao, B. chen, A. Miner, S. Priya, Low thermal conductivity of Al-doped ZnO with layered and correlated grains, RSC Adv. 4 (2014) 18370.
[32] G. Klirat, M.A. Aksan, S. Rasekh, M.A. Madre, J.C. Diez, A. Sotelo, Decrease of $Ca_3Co_4O_{9+\delta}$ thermal conductivity by Yb-doping, Ceram. Int. 41 (2015) 12529–12534.
[33] R.V. Rivera Virtudazo, Q. Guo, R. Wu, T. Takei, T. Mori, An alternative, faster and simpler method for the formation of hierarchically porous ZnO particles and their thermoelectric performance, RSC Adv. 7 (2017) 31960.
[34] C. Chen, F. Giovannelli, F. Delorme, Thermoelectric properties of $Fe_{2-x}Ti_{1+x}O_5$ pseudobrookite ceramics: influence of microcracking and Nb substitution, Ceram. Int. 44 (2018) 21794–21799.
[35] F. Giovannelli, C. Chen, P. Diaz-Chao, E. Guilmeau, F. Delorme, Thermal conductivity and stability of Al-doped ZnO nanostructured ceramics, J. Eur. Ceram. Soc. 38 (2018) 5015–5020.
[36] A. Sotelo, M. Depriester, M.A. Torres, A.H. Sahraoui, M.A. Madre, J.C. Diez, Effect of simultaneous K, and Yb substitution for Ca on the microstructural and thermoelectric characteristics of $CaMnO_3$ ceramics, Ceram. Int. 44 (2018) 12697–12701.
[37] F. Delorme, R. Dujardin, F. Schoenstein, B. Pintault, P. Belleville, C. Autret, I. Monot-Laffez, F. Giovannelli, Nanostructuring of dense SnO_2 ceramics by spark plasma sintering, Ceram. Int. 45 (2019) 8313–8318.
[38] M. Wolf, K. Menekse, A. Mundstock, R. Hinterding, F. Nietschke, O. Oekler, A. Feldhoff, Low thermal conductivity in thermoelectric oxide-based multiphase composites, J. Electron. Mater. 48 (2019) 7551–7561.
[39] L.L. Chen, Z.Y. Zhang, N. Qi, B. Zhou, S.P. Deng, Z.Q. Chen, Y.C. Wu, X.F. Tang, Giant reduction in thermal conductivity of Co_3O_4 with ordered mesopore structures, Microporous Mesoporous Mater. 296 (2020), 109969.
[40] H.-W. Son, Q. Guo, Y. Suzuki, B.-N. Kim, T. Mori, Thermoelectric properties of $MgTi_2O_5$/TiN conductive composites prepared via reactive spark plasma sintering for high temperature functional applications, Scr. Mater. 178 (2020) 44.
[41] Y. Saito, H. Takao, T. Tani, T. Nonoyama, K. Takatori, T. Homma, T. Nagaya, M. Nakamura, Lead-free piezoceramics, Nature 432 (2004) 84–87.
[42] J. Rödel, W. Jo, K.T.P. Seifert, E.-A. Anton, T. Granzow, D. Damjanovic, Perspective on the development of lead-free piezoceramics, J. Am. Ceram. Soc. 92 (2009) 1153–1177.
[43] C.R. Bowen, H.A. Kim, P.M. Weaver, S. Dunn, Piezoelectric and ferroelectric materials and structures for energy harvesting applications, Energy Environ. Sci. 7 (2014) 25–44.
[44] J. Wu, D. Xiao, J. Zhu, Potassium-sodium niobate lead-free piezoelectric materials: past, present, and future of phase boundaries, Chem. Rev. 115 (2015) 2559–2595.
[45] M. Bah, F. Giovannelli, F. Schoenstein, G. Feuillard, E. Le Clezio, I. Monot-Laffez, High electromechanical performance with spark plasma sintering of undoped $K_{0.5}Na_{0.5}NbO_3$ ceramics, Ceram. Int. 40 (2014) 7473–7480.
[46] F. Delorme, M. Bah, F. Schoenstein, F. Jean, M. Zouaoui Jabli, I. Monot-Laffez, F. Giovannelli, Thermoelectric properties of oxygen deficient $(K_{0.5}Na_{0.5})NbO_3$ ceramics, Mater. Lett. 162 (2016) 24–27.
[47] S.R. Popuri, A.J.M. Scott, R.A. Downie, M.A. Hall, E. Suard, R. Decourt, M. Pollet, J.-W.G. Bos, Glass-like thermal conductivity in $SrTiO_3$ thermoelectrics induced by A-site vacancies, RSC Adv. 4 (2014) 33720.
[48] A.V. Kovalevsky, A.A. Yaremchenko, S. Populoh, A. Weidenkaff, J.R. Frade, Effect of A-site cation deficiency on the thermoelectric performance of donor-substituted strontium titanate, J. Phys. Chem. C 118 (2014) 4596–4606.

[49] Z. Lu, H. Zhang, W. Lei, D.C. Sinclair, I.M. Reaney, High-figure-of-merit thermoelectric La-doped A-site-deficient SrTiO3 ceramics, J. Chem. Mater. 28 (2016) 925–935.
[50] B. Jaffe, W.R. Cook, H. Jaffe, Piezoelectric Ceramics, Academic Press, London, 1971.
[51] M. Bah, N. Alyabyeva, R. Retoux, F. Giovannelli, M. Zaghrioui, A. Ruyter, F. Delorme, I. Monot-Laffez, Investigation of the domain structure and hierarchy in potassium–sodium niobate lead-free piezoelectric single crystals, RSC Adv. 6 (2016) 49060–49067.
[52] T. Wada, K. Tsuji, T. Saito, Y. Matsuo, Ferroelectric $NaNbO_3$ ceramics fabricated by spark plasma sintering, J. Appl. Phys. 42 (2003) 6110–6114.
[53] N. Shomrat, S. Baltianski, C.A. Randall, Y. Tsur, Flash sintering of potassium-niobate, J. Eur. Ceram. Soc. 35 (2015) 2209–2213.
[54] G. Gouget, F. Mauvy, U.-C. Chung, S. Fourcade, M. Duttine, M.-D. Braida, T. Le Mercier, A. Demourgues, Associating and tuning sodium and oxygen mixed-ion conduction in niobium-based perovskites, Adv. Funct. Mater. 30 (2020), 1909254.
[55] M.R. Winter, D.R. Clarke, Oxide materials with low thermal conductivity, J. Am. Ceram. Soc. 90 (2007) 533–540.
[56] R. Taylor, J.R. brandon, P. Morrell, Microstructure, composition and property relationships of plasma-sprayed thermal barrier coatings, Surf. Coat. Technol. 50 (1992) 141–149.
[57] A.G. Evans, D.R. Mumm, J.W. Hutchinson, G.H. Meier, F.S. Pettit, Mechanisms controlling the durability of thermal barrier coatings, Prog. Mater. Sci. 46 (2001) 505–553.
[58] X.Q. Cao, R. Vassen, D. Stoever, Ceramic materials for thermal barrier coatings, J. Eur. Ceram. Soc. 24 (2004) 1–10.
[59] A.M. Hofmeister, Thermal diffusivity of oxide perovskite compounds at elevated temperature, J. Appl. Phys. 107 (2010), 103532.
[60] M. Tachibana, T. Kolodiazhnyi, E. Takayama-Muromachi, Thermal conductivity of perovskite ferroelectrics, Appl. Phys. Lett. 93 (2008), 092902.
[61] Y.I. Yuzyuk, P. Simon, E. Gagarina, L. Hennet, D. Thiaudiere, V.I. Torgashev, S. I. Raevskya, I.P. Raevskii, L.A. Reznitchenko, J.L. Sauvajol, Modulated phases in $NaNbO_3$: raman scattering, synchrotron x-ray diffraction, and dielectric investigations, J. Phys. Condens. Matter 17 (2005) 4977–4990.
[62] Y. Shiratori, A. Magrez, W. Fischer, C. Pithan, R. Waser, Temperature-induced phase transitions in micro-, submicro-, and nanocrystalline $NaNbO_3$, J. Phys. Chem. C 111 (2007) 18493–18502.
[63] S.K. Mishra, R. Mittal, V.Y. Pomjakushin, S.L. Chaplot, Phase stability and structural temperature dependence in sodium niobate: a high-resolution powder neutron diffraction study, Phys. Rev. B 83 (2011), 134105.
[64] G. Xing, J. Sun, K.P. Ong, X. Fan, W. Zheng, D.J. Singh, Perspective: n-type oxide thermoelectrics via visual search strategies, APL Mater. 4 (2016), 053201.